Developmental Cognitive Neuroscience 46 (2020) 100875

Contents lists available at ScienceDirect

Developmental Cognitive Neuroscience

journal homepage: www.elsevier.com/locate/dcn

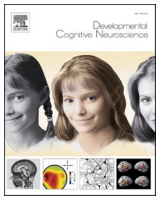

Grey and white matter volumes in early childhood: A comparison of voxel-based morphometry pipelines

Logan Haynes [a,b,c], Amanda Ip [a,b,c,e], Ivy Y.K. Cho [a,b,c], Dennis Dimond [a,b,d,e], Christiane S. Rohr [a,b,c,e], Mercedes Bagshawe [a,b,c], Deborah Dewey [a,b,f,g,h], Catherine Lebel [a,b,c,e], Signe Bray [a,b,c,e,*]

[a] Child and Adolescent Imaging Research Program, University of Calgary, Calgary, Canada
[b] Alberta Children's Hospital Research Institute, University of Calgary, Calgary, Canada
[c] Department of Radiology, Cumming School of Medicine, University of Calgary, Calgary, Canada
[d] Department of Neuroscience, Cumming School of Medicine, University of Calgary, Calgary, Canada
[e] Hotchkiss Brain Institute, University of Calgary, Calgary, Canada
[f] Department of Paediatrics, Cumming School of Medicine, University of Calgary, Calgary, Canada
[g] Department of Community Health Sciences, University of Calgary, Calgary, Canada
[h] Owerko Centre, University of Calgary, Calgary, Canada

ARTICLE INFO

Keywords:
Voxel-based morphometry
Early childhood
MRI
Development

ABSTRACT

Early childhood is an important period of sensory, motor, cognitive and socio-emotional maturation, yet relatively little is known about the brain changes specific to this period. Voxel-based morphometry (VBM) is a technique to estimate regional brain volumes from magnetic resonance (MR) images. The default VBM processing pipeline can be customized to increase accuracy of segmentation and normalization, yet the impact of customizations on analyses in young children are not clear. Here, we assessed the impact of different preprocessing steps on T1-weighted MR images from typically developing children in two separate cohorts. Data were processed with the Computational Anatomy Toolbox (CAT12), using seven different VBM pipelines with distinct combinations of tissue probability maps (TPMs) and DARTEL templates created using the Template-O-Matic, and CerebroMatic. The first cohort comprised female children aged 3.9–7.9 years (N = 62) and the second included boys and girls aged 2.7–8 years (N = 74). We found that pipelines differed significantly in their tendency to classify voxels as grey or white matter and the conclusions about some age effects were pipeline-dependent. Our study helps to both understand age-associations in grey and white matter volume across early childhood and elucidate the impact of VBM customization on brain volumes in this age range.

1. Introduction

Characterizing brain development in early childhood is critical to understanding the profound cognitive and emotional maturation occurring across this period. Much of what is known about early childhood brain development comes from studies that include wide age ranges (Sowell et al., 2004; Walhovd et al., 2017; Krongold et al., 2017), with few studies describing changes specific to this period (Brown and Jernigan, 2012). With more focused sampling in early childhood, we can begin to precisely characterize brain changes in this important developmental period.

From models fit to wider age ranges, it is understood that there is thinning of the cortex (Walhovd et al., 2017), and volumetric white matter expansion (Bray et al., 2015; Lebel and Beaulieu, 2011), across childhood and adolescence. Using software that fits a model to the pial and white matter surfaces (Fischl, 2012; Kabani et al., 2001), the volume of the cortex can be decomposed into thickness and surface area. Although there are some inconsistencies in the literature (described in (Walhovd et al., 2017)), it is now generally agreed that from at least the preschool period onwards, cortical thickness changes are dominated by thinning (Krongold et al., 2017; Wierenga et al., 2014; Mills et al., 2014; Zielinski et al., 2014; Brown et al., 2012). Thinning has been shown to be relatively slow and protracted in prefrontal regions, and more rapid at an earlier age in posterior regions (Brown and Jernigan, 2012). The

* Corresponding author at: 28 Oki Drive, ACH B4-514, Calgary, AB, T3B 6A8, Canada.
E-mail address: slbray@ucalgary.ca (S. Bray).

https://doi.org/10.1016/j.dcn.2020.100875
Received 29 July 2019; Received in revised form 10 September 2020; Accepted 21 October 2020
Available online 24 October 2020
1878-9293/© 2020 The Authors. Published by Elsevier Ltd. This is an open access article under the CC BY-NC-ND license (http://creativecommons.org/licenses/by-nc-nd/4.0/).

nature of thickness changes remains poorly understood, with some work suggesting it is related primarily to increased myelination of the deep cortical layers rather than thinning of the grey matter per se (Natu et al., 2019). In childhood, surface area develops on a separate and partially independent trajectory relative to thickness 9], showing region-specific increases that reach a peak in late childhood/early adolescence (Krongold et al., 2017; Wierenga et al., 2014). Most of these studies sampled down to age 7, with some sampling as young as 3 or 4 years of age (Krongold et al., 2017; Zielinski et al., 2014; Brown et al., 2012).

Volumetric studies generally show what while there is minimal change in total brain volume from the age of 4–18, there are parallel relative increases in white matter volume into adulthood and relative decreases in grey matter volume (Brain Development Cooperative Group, 2012; Jernigan et al., 1991; Lebel et al., 2012). Cortical volume can be estimated as the product of surface area and thickness extracted from surface-based methods. Another commonly used method for studying regional volumes is voxel-based morphometry (VBM) (Pergher et al., 2019; Weise et al., 2019; Chen et al., 2018; Ashburner and Friston, 2000; Douaud et al., 2007), an automated analysis technique that can be used to identify volumetric differences between groups, or associations with age, through voxel-wise statistical comparisons (Ashburner and Friston, 2000). VBM is less labour-intensive than other techniques such as manual tracing, and allows for unbiased analysis that is not restricted to *a priori* regions of interest (Whitwell, 2009). Furthermore, VBM has been shown to generally approximate the results of manual volumetry, suggesting reasonable methodological validity (Asami et al., 2012; Bergouignan et al., 2009; Focke et al., 2014). A further strength of VBM is that it allows parallel examination of regional cortical, subcortical and cerebellar grey matter as well as white matter volumes (Bray et al., 2015; D'Mello et al., 2016).

Volumetric studies of cortical grey matter have shown regionally varying negative associations with age across childhood, coupled with positive white matter volume associations (Brain Development Cooperative Group, 2012; Taki et al., 2013; Lenroot et al., 2007). Across adolescence, more rapid volume decline in prefrontal and parietal lobes, relative to temporal and occipital lobes has been shown (Brain Development Cooperative Group, 2012; Lenroot et al., 2007), though other voxel-wise work in children aged 7–23 has suggested more substantial maturation in parietal and temporal regions (Guo et al., 2007). A previous combined GM and WM VBM analysis from our group showed increases in some prefrontal and cerebellar gray matter regions in early childhood (4–8 years) and consistent declines in volume thereafter, coupled with white matter volume increases that were relatively consistent across regions, but showed spatially specific patterns. In addition to normative age associations, VBM analyses have been widely applied to study neurodevelopmental conditions (D'Mello et al., 2015, 2016; Bray et al., 2011; Hoeft et al., 2008; Xia et al., 2016).

A challenge in implementing VBM analyses, however, is the wide array of available processing options and a lack of clarity on the best approach to optimize processing of data from groups other than neurotypical adults. A standard VBM workflow includes segmentation and normalization steps, both of which can be customized in different ways. The default segmentation template provided by SPM, a commonly used implementation of the VBM approach, reflects the probability of tissue classification in the average adult brain. Furthermore, the default normalization procedure involves warping images to a diffeomorphic anatomical registration through an exponentiated lie algebra (DARTEL) (Ashburner, 2007) template. This default DARTEL template is derived from a population of healthy adult brains (n = 555; mean age ~48 years) from the Information eXtraction from Images (IXI) study (https://brain-development.org/) (Gaser and Kurth, 2018). It has been acknowledged that these default parameters may not be ideal for analyzing populations whose neuroanatomy deviates from these reference standards, such as young children (Kurth et al. (2015); Altaye et al. (2008)). However, with a growing number of available options for VBM preprocessing (Wilke et al., 2017; Wilke, 2018; Wilke et al., 2008), work is needed to establish trade-offs and support decision-making for pipeline use in early childhood studies.

The present work compares the outputs from different VBM pipelines in order to determine how pipeline choice impacts tissue classification, normalization and statistical inferences. To this end, we evaluated seven different VBM processing pipelines on two early childhood cohorts, including a sample of 62 girls aged 3.9–7.9 and a separate sample of 74 boys and girls aged 2.9–6.9 years. Our findings can support investigators in their selection of processing approaches for VBM studies and also shed new light on the volumetric brain changes occurring in early childhood.

2. Methods

2.1. Pipeline customization options

In VBM processing, T1-weighted images are first segmented into grey and white matter images of voxel-wise tissue probabilities. The segmentation of T1 images into different tissue classes is influenced by a tissue prior, also known as a tissue probability map (TPM). Individual grey and white matter images are warped to fit a common DARTEL template (Klein et al., 2009). Normalized images are subsequently modulated to preserve the initial amount of grey and white matter present in each voxel prior to their spatial warping. Smoothing is then performed to mitigate between-participant differences in spatial normalization and to satisfy the assumptions of parametric statistical testing (Ashburner and Friston, 2000). Two places where study-specific customization becomes possible are 1) creating custom TPMs and 2) creating custom DARTEL templates.

2.1.1. Custom TPMs

Custom TPMs can be created in the Template-O-Matic toolbox (TOM8: http://www.neuro.uni-jena.de/software/tom/) (Wilke et al., 2008). This approach uses the US National Institute of Health's (NIH) MRI Study of Normal Brain Development and general linear models to assess how demographic variables affect the brain structures of 404 children aged 5–18 (Wilke et al., 2008). Using the model fits, custom TPMs can then be created by matching these regression parameters to the demographics of a pediatric population of interest (Wilke et al., 2008). However, the fit may not be appropriate for children outside this age range.

The CerebroMatic toolbox (COM: https://www.medizin.uni-tuebingen.de/kinder/en/research/neuroimaging/software/) (Wilke et al., 2017) is a second option for generating custom TPMs that matches sample demographics to parameters that influence brain structure using a flexible non-parametric approach: multivariate adaptive regression splines (Wilke et al., 2017). In CerebroMatic, the regression parameters are modelled using 1914 healthy participants aged 13 months to 75 years, providing broader applicability across age ranges than TOM8 (Wilke et al., 2017). The cohort used to model regression parameters includes pediatric scans from the NIH Study of Normal Brain Development, and the Cincinnati MR Imaging of Neurodevelopment study (C-MIND). Adult scans were acquired through the 1000 functional connectome study (fCONN) and the IXI database (Wilke et al., 2017). Note that with a sufficiently large sample, a custom template could also be created from study participants; however, that option was not examined here.

2.1.2. Custom DARTEL templates

Normalization can be customized using DARTEL templates (Gaser and Kurth, 2018). Study-specific DARTEL templates can be created using the segmented TPMs of all study participants. These partial volume images are then used in a subsequent template creation step, and the newly created DARTEL template can be registered to standard Montreal Neurological Institute (MNI) space. Notably, the use of segmented images in the template creation step means that the DARTEL template is inherently influenced by the upstream segmentation process, including

Table 1
VBM Pipeline Combinations. All preprocessing steps remained the same between iterations, but each pipeline used a different combination of tissue probability map and DARTEL template.

Pipeline	Tissue Probability Map (TPM)	DARTEL Template
1	Default	Default
2	Default	Custom CAT12
3	Custom Template-O-Matic (TOM8)	Default
4	Custom Template-O-Matic (TOM8)	Custom CAT12
5	Default	Custom CerebroMatic (COM)
6	Custom CerebroMatic (COM)	Default
7	Custom CerebroMatic (COM)	Custom CerebroMatic (COM)

the choice of TPM.

A second option for creating DARTEL templates is CerebroMatic, which matches sample demographics to a second set of regression parameters derived from 1919 participants in the same databases (Wilke, 2018). To generate these DARTEL-specific regression parameters, CerebroMatic used SPM tools to create a custom DARTEL template for their dataset, while monitoring the effects of each individual registration by extracting intermediary deformation fields throughout the template creation process. This allowed for modeling the effects of participant demographics on DARTEL templates, generating regression parameters that can then be matched to other participant samples.

2.1.3. Selected pipelines and preprocessing

All image preprocessing was performed using the Computational Anatomy Toolbox (CAT12: http://dbm.neuro.uni-jena.de/cat/), run through SPM12 in MATLAB (9.2). Seven different preprocessing pipelines were assessed that each contained a distinct combination of TPM and DARTEL templates (Table 1). Aside from these variations, all other CAT12 default settings were kept constant across pipelines. All pipelines included affine regularisation to the European ICBM template, rough affine preprocessing, and 1.5 mm normalized isotropic voxels. Inhomogeneity correction, local adaptive segmentation strength, skull stripping, and final cleanup strength were set to medium. Each of the pipelines below produced normalized grey and white matter images modulated to preserve the amount of grey and white matter, which were then smoothed with an 8 mm FWHM Gaussian kernel. The distinct TPM and DARTEL combinations used in the 7 preprocessing pipelines were as follows:

1) Default TPM / Default DARTEL Pipeline

In this pipeline, images were preprocessed using CAT12 default settings, which included the default TPM from SPM, and the default DARTEL template (derived from 555 healthy adult controls in the IXI-database).

2) Default TPM / Custom DARTEL Pipeline

Affine-registered grey and white matter segmentations were exported from CAT12 using default settings and subsequently used for SPM DARTEL template creation. This custom DARTEL template was then normalized to MNI space.

3) Template-O-Matic TPM / Default DARTEL Pipeline

A custom TPM was generated in the TOM8 toolbox using the 'average approach' based on the average participant demographics. We note that the alternative matched pairs approach was not feasible, as our sample included children younger than 5 years, which is the minimum age of participants in the sample used to develop the TOM8 toolbox (Wilke et al., 2008). This pipeline used the default DARTEL template.

4) Template-O-Matic TPM / Unbiased Custom DARTEL Pipeline

Images were first segmented using an age/sex-matched Template-O-Matic TPM with a default DARTEL template. During this preprocessing, the affine DARTEL export function was used to generate grey and white matter segmentations. These affine segments were then used to create a new custom DARTEL template for the sample, which was then normalized to MNI space. Thus, unlike pipeline #2, this template was created from image segments obtained using an age-appropriate TPM.

5) Default TPM / CerebroMatic DARTEL Pipeline

The age and sex of participants, and field strength were entered into the CerebroMatic toolbox to create a custom template. This CerebroMatic DARTEL template was used with a default TPM.

6) CerebroMatic TPM / Default DARTEL Pipeline

The same demographic variables from our pediatric cohort were supplied to the CerebroMatic toolbox, and a custom TPM was generated using the toolbox's unified segmentation parameters. T1 images were preprocessed using this custom TPM and the default DARTEL template.

7) CerebroMatic TPM / CerebroMatic DARTEL Pipeline

The custom DARTEL and TPM generated in CerebroMatic were combined into a single pipeline for the preprocessing of all T1 images.

Note that two additional possible TPM and DARTEL combinations were not explored: Template-O-Matic TPM / CerebroMatic DARTEL and CerebroMatic TPM/ custom DARTEL. We assumed that investigators using CerebroMatic would apply its full capacity rather than combining with older options for customization.

2.2. Characterizing differences between pipelines

2.2.1. Participants, MRI data collection and selection of T1 images

For this study, two sets of data from two independent studies conducted at the same site were used in parallel analyses in order to understand whether variations in tissue segmentation and normalization between pipelines were consistent.

2.2.1.1. Cohort 1. T1-weighted structural MR images were collected at the Alberta Children's Hospital from 78 typically developing female children aged 3.9–7.9 years. Pre-screening ensured that participants were not born earlier than 37 weeks gestation and had no psychiatric or neurological diagnoses. Parents reported their child's preferred handedness on a five-point scale ranging from mainly left- to mainly right-handed. Handedness was coded as a binary left- or right- handed and no parents reported that their child was fully ambidextrous. A subset of participants also received follow-up scans after 6 and/or 12 months, leaving many participants with multiple scans available at the time of analysis. For each participant one image with the highest quality based on visual inspection was chosen for analyses, as described in more detail below. MR images were collected at the Alberta Children's Hospital on a 3 T GE MR750w (Waukesha, WI) scanner with a 32-channel head coil. A T1-weighted 3D BRAVO sequence was used to obtain anatomical scans (TR =6.764 ms, TE =2.908 ms, FA = 10, FOV = 240 × 240, matrix = 300 × 300, voxel size 0.8 × 0.8 × 0.8 mm^3). Images were visually inspected for motion artifacts and assigned an overall quality rating based on comparison to 5 exemplar images of differing levels of quality (Supplementary Figure S1). Specifically, the exemplar for a rating of 5 clearly shows the details of anatomical structure with no obvious artifact, and exemplars from levels 4 to 1 showing increasing amounts of ringing such that at levels 2 and 1 it is difficult to distinguish anatomical boundaries. For each participant with multiple scans, the highest quality image was retained. Participants whose highest quality image received a rating of poor (score of 1 or 2) were excluded, and 1 participant was

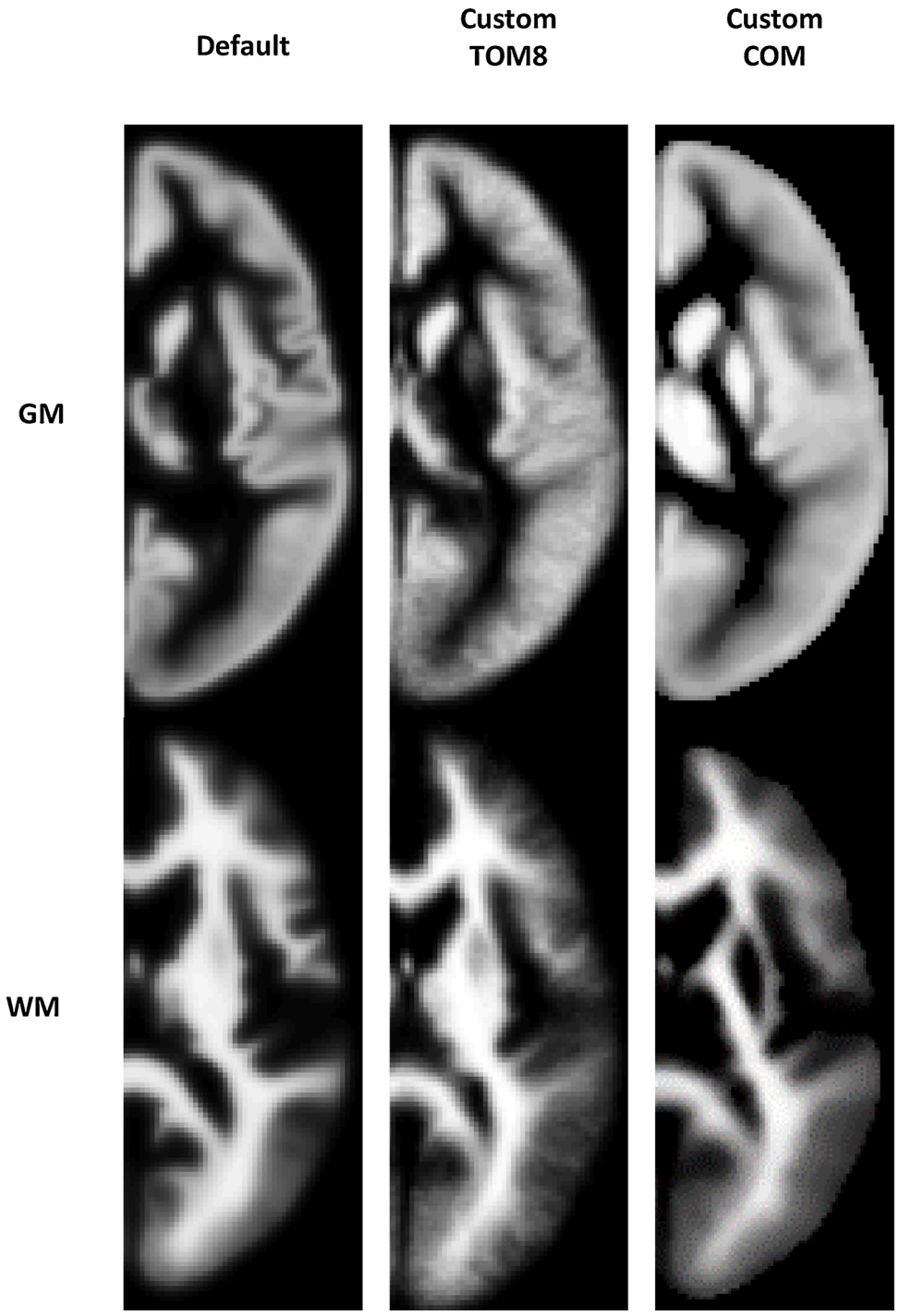

Fig. 1. Grey and white matter TPMs in cohort 1. TPMs were similar to one another but notably the default template has sharper definition of tissue probability relative to the custom templates. The CerebroMatic grey matter TPMs had higher intensity at the edge of the brain. It is also notable that in the Default and TOM8 TPMs, relative to COM, subcortical structures are incorrectly classified as white matter. Although only grey and white matter tissue classes are shown, each 6-volume TPM also included a cerebrospinal fluid volume, and 3 background classes.

excluded due to an incidental finding. Following this process, 62 images were retained for further analysis (aged 3.89–7.89 years; $\bar{x} = 5.69$ years; sd = 0.94 years; 5 left-handed).

2.2.1.2. Cohort 2. Structural MR images were obtained from a second cohort of 114 male and female children aged 2.9–6.9 years as part of a separate study at the Alberta Children's Hospital using the same MRI scanner and 32 channel head coil. All children were free of diagnosed psychiatric or neurodevelopmental disorders. After scanning at baseline, participants were invited for repeat scans every 6 months, leaving multiple scans per participant available at the time of analysis. T1-weighted images were acquired with an FSPGR BRAVO sequence (flip angle = 12°, 210 slices, TR = 8.23 ms, TE = 3.76 ms, voxel size = 0.9 × 0.9 × 0.9mm^3, matrix size = 512 × 512, inversion time = 540 ms). Images underwent quality assessment using the scoring scale outlined above. A total of 74 participants had at least one high quality scan. Only one scan per participant was used in the cross-sectional analyses described here (aged 2.7–8.0 years; $\bar{x} = 4.61$ years; sd = 1.1 years; 38 males; 7 left-handed).

2.2.2. Pipeline comparison

2.2.2.1. Comparison of brain volume estimates. Total intracranial (TIV), grey matter, and white matter volumes were estimated for each

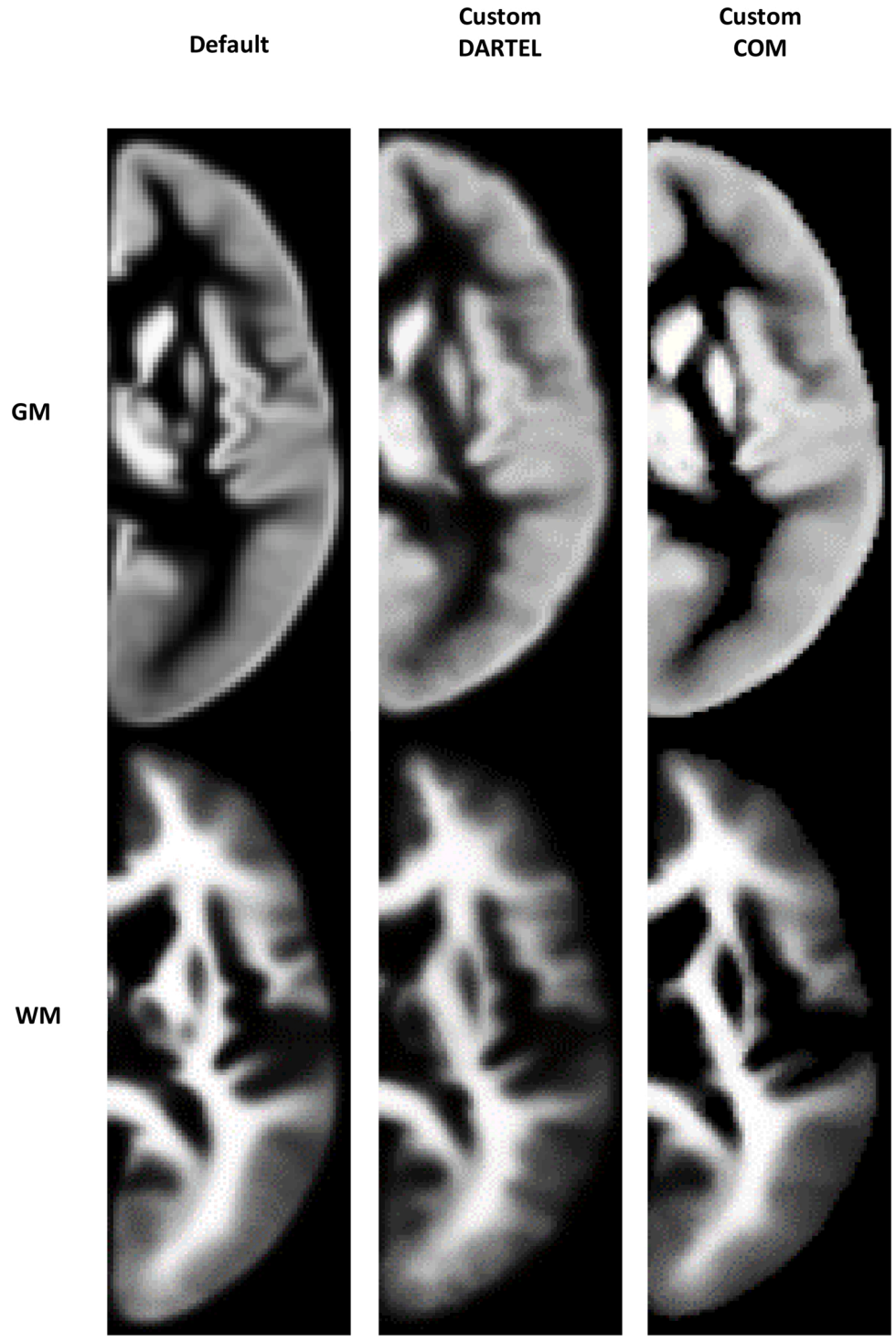

Fig. 2. Grey and white matter DARTEL templates for cohort 1. Similar to the TPM, the CerebroMatic grey matter DARTEL template had higher intensity at the edge of the brain and sharper definition of subcortical structures.

participant. These estimates were compared using R 3.6.3 across all three segmentation options using a repeated-measures ANOVA and pairwise t-tests to assess differences between pipelines.

2.2.2.2. TPM impact on tissue segmentations. Individual participants' native-space grey matter segmentations from different pipelines were overlaid onto their T1 image for visual inspection of regions where tissue classification differed between the Template-O-Matic and CerebroMatic custom TPM options. In order to assess systematic differences in tissue classification for different TPMs, general linear models (GLM) in SPM12 were generated with TPM as the within-subject factor, and paired *t*-test contrasts. These models compared TPM influence on pipelines using the default DARTEL template.

2.2.2.3. Effects of DARTEL template on spatial normalization. Paired *t*-test models were conducted to compare the outputs of pipelines with different DARTEL templates, while using the default TPM as a constant.

Table 2
Pairwise comparisons of mean volumetric outputs for different TPMs in cohort 1. Paired t-tests were used to compare tissue volume estimates between pairs of pipelines. TPM = tissue probability map, TOM = Template-O-Matic, COM = CerebroMatic.

Measure: TIV						
TPM 1 (cm^3)	TPM 2 (cm^3)	Mean Difference	t(61)	P-value	95 % Confidence Interval for Difference †	
					Lower Bound	Upper Bound
Default (1385.12)	TOM (1400.61)	−15.49	−7.08	<0.001	−19.87	−11.12
Default (1385.12)	COM (1379.02)	6.10	2.76	0.008	1.68	10.52
TOM (1400.61)	COM (1379.02)	21.59	12.59	<0.001	18.16	25.02
Measure: GM Volume						
TPM 1 (cm^3)	TPM 2 (cm^3)	Mean Difference	t(61)	P-value	95 % Confidence Interval for Difference †	
					Lower Bound	Upper Bound
Default (750.34)	TOM (757.73)	−7.38	−3.96	<0.001	−11.11	−3.66
Default (750.34)	COM (754.82)	−4.48	−1.94	0.06	−9.09	0.13
TOM (757.73)	COM (754.82)	2.90	1.54	0.13	−0.88	6.68
Measure: WM Volume						
TPM 1 (cm^3)	TPM 2 (cm^3)	Mean Difference	t(61)	P-value	95 % Confidence Interval for Difference †	
					Lower Bound	Upper Bound
Default (417.74)	TOM (425.69)	−7.95	−14.43	<0.001	−9.05	−6.84
Default (417.74)	COM (416.30)	1.44	2.76	.008	0.40	2.48
TOM (425.69)	COM (416.30)	9.39	19.80	<0.001	8.44	10.34

2.2.2.4. Comparison of pipeline sensitivity to age effects. A set of GLMs were run to assess and qualitatively compare linear associations with age in grey and white matter volume estimates from each pipeline. While studies over wider age ranges have shown some non-linear associations between age and regional volumes (Wierenga et al., 2014; Taki et al., 2013), linear effects were assessed given the relatively narrow age range and cross-sectional measurements. In order to estimate age effects as accurately as possible, data were pooled across the two cohorts for this analysis. Models included age as the regressor of interest, and total intracranial volume (TIV), sex, handedness and cohort were included as covariates. TIV was included as a covariate rather than as a scaling factor because it has been shown that different brain regions scale differently with global volume (Reardon et al., 2018). TIV was controlled for in two different ways in separate analyses. In the first, the TIV estimate generated for each pipeline was included in the respective analysis. This is the method most likely to be used in practice, and thus has higher external validity. However, because this means that differences in results between pipelines could be due either to differences in the processed images or due to the use of a different covariate, a second set of analyses was run using consistent TIV values from the default segmentation. For the purpose of comparing pipelines, the number of grey and white matter voxels that were associated with age at an uncorrected height threshold of $\alpha = 0.001$ were tabulated for each pipeline. We also ascertained significant age associations for each pipeline (using pipeline-specific TIV covariates) using a height threshold of $\alpha < 0.001$ and cluster-level corrected for family-wise error at $\alpha < 0.05$. Significant cortical regions were anatomically labeled according to the Harvard-Oxford atlas (Desikan et al., 2006) and white matter regions using the JHU atlas (Wakana et al., 2007; Hua et al., 2008).

3. Results

3.1. Pipeline comparison

3.1.1. Visual comparison of TPMs and DARTEL templates

Visual comparisons of the three grey and white matter TPMs and DARTEL templates used across pipelines are shown for cohort 1 in Figs. 1 and 2 (observations were similar in cohort 2). TPMs were similar to one another, but notably the default template has sharper definition of tissue probability relative to the custom templates. The CerebroMatic grey matter TPM and DARTEL templates had higher intensity at the edge of the brain. It can be seen that the CerebroMatic TPM has more accurate delineation of subcortical grey and white matter, relative to the default and TOM8 TPMs which classify sub-cortical grey matter in the putamen as white matter.

3.1.2. TPM selection affects volume estimates

In both cohorts, tissue classification estimates showed significant differences depending on pipeline. In cohort 1 (Tables 1 and 2), we found a significant effect of pipeline on estimates of TIV ($F(2,122) = 58.95$, $p < .001$), GM ($F(2,122) = 6.71$, $p < 0.002$) and WM ($F(2,122) = 191.81$, $p < .001$). In cohort 2 (Table 2), we also found a significant effect of pipeline on estimates of TIV ($F(2,146) = 65.8$, $p < 0.001$), GM ($F(2, 146) = 31.84$, $p < 0.001$) and WM ($F(2, 146) = 76.2$, $p < 0.001$). In cohort 1, the TOM8 TPM resulted in the largest TIV, followed by the default TPM and the CerebroMatic TPM. In cohort 2, both TOM8 and COM pipelines resulted in larger TIV estimates, relative to the default. Across both cohorts, the TOM8 TPM produced the largest white matter estimates. COM produced the largest grey matter estimate for cohort 2, while it produced the smallest grey matter estimate for cohort 1, though in cohort 1 the COM estimate was not significantly smaller than the TOM8 or default estimate (Table 2). Across the two cohorts, relative volume differences between pipelines were more consistent for the TOM8 TPM (greater GM and WM volumes), whereas the CerebroMatic TPM resulted in less consistent differences in volume estimates, relative to the default TPM.

3.1.3. TPM selection affects tissue classification

Paired t-tests comparing the outputs from pipelines using different TPMs identified regions of significant difference between pipelines (Fig. 3). Relative to default, TOM8 TPM led to increased grey matter concentration in medial prefrontal, occipital and temporal regions, and reduced GM in the striatum and thalamus. The COM TPM led to increased grey matter in sub-cortical regions, as would be expected based on the differences in TPMs in subcortical structures, as well as occipital and dorsal prefrontal regions. For white matter, TOM8 increased the classification of deep white matter, cerebellar white matter and superficial regions in prefrontal and occipital lobes. COM8 led to decreased classification of deep white matter near the striatum and increased classification in diffuse regions and the cerebellum.

When comparing the effect of DARTEL template (Fig. 4), we found that, for grey matter, both custom DARTEL templates led to increased

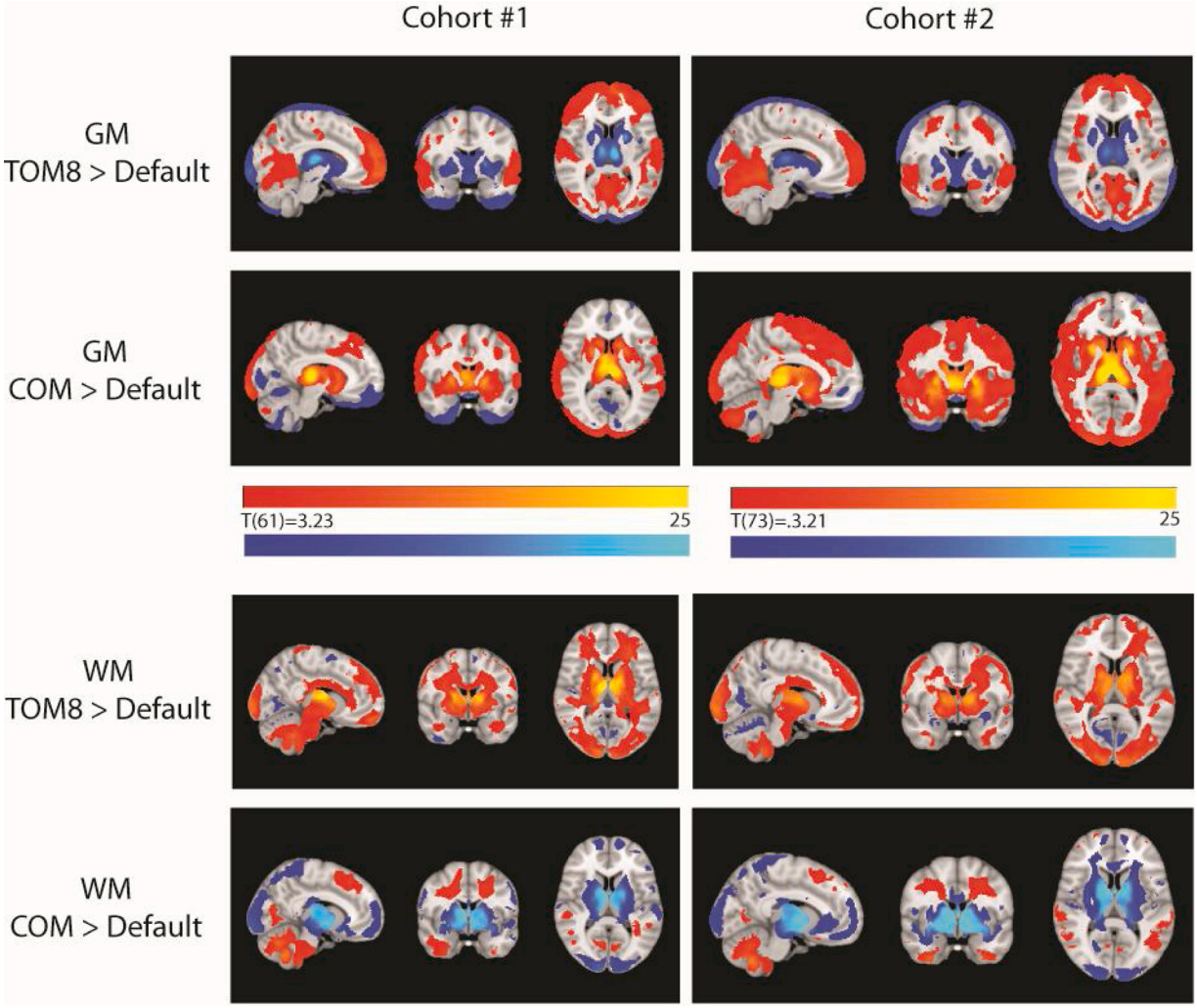

Fig. 3. Significant differences in tissue classification based on TPM. Within each cohort, paired t-tests compared grey matter (GM) and white matter (WM) images from pipelines using different TPMs, all using the default DARTEL template. TPMs differentially altered tissue classification in a relatively consistent way across the two cohorts, but choice of TPM impacted classification in deep white and grey matter regions as well as across cortical regions. Slices shown at [-9 -1 9]; display is radiological. TOM8=Template-o-Matic 8, COM = CerebroMatic.

grey matter concentration at the periphery of the cortex and reduced concentration in deep white matter regions. For white matter, custom DARTEL templates consistently increased concentration of relatively superficial white matter (Table 3). Overall, differences were relatively consistent across customization options and across the two cohorts.

3.1.4. Pipelines show different sensitivity to age associations

Models across all pipelines showed linearly decreasing grey matter volumes and increasing white matter with age, as expected. As there were no significant clusters showing the opposite pattern, we focus on those two contrasts here: positive age associations for white matter and negative age associations for grey matter. The numbers of voxels exceeding a statistical threshold of $p < 0.001$ are shown in Fig. 5a (pipeline specific TIV covariate) and 5b (consistent default segmentation TIV covariate). This figure shows that the choice of TPM seemed to have the larger impact on the number of significant voxels than DARTEL template, and this remained true when using a fixed TIV covariate (5b). In the models with pipeline-specific covariates, for both grey and white matter analyses the TOM8 TPM showed the largest number of significant voxels, followed by the default pipeline and COM. For the models with a fixed TIV, TOM8 showed the most significant grey matter voxels and an intermediate number of significant white matter voxels. In general, pipeline differences in the number of significant voxels were related to both changes in cluster size and changes in the number of significant clusters, though changes in cluster size appeared to be the dominant change.

Figs. 6 and 7 illustrate differences across pipelines using the three different TPMs from models using the pipeline-specific covariate (i.e. represented in Fig. 5a), all using the default DARTEL template. Tables of significant values for these models are included in the Supplementary Material and it can be seen in Supplementary Tables 1–6 that the size of significant clusters varied substantially across pipelines, as well as the number of clusters reaching corrected significance. For grey matter analyses, across pipelines we found significant clusters in left lateral occipital cortex, medial frontal and medial and lateral orbitofrontal cortices (Fig. 6). In the default and TOM8 segmented analyses, there were additional significant clusters in right lateral occipital cortex, precuneus and left superior occipital regions. We did not find significant clusters in these latter regions in the COM analysis.

For white matter analyses, across pipelines we found a large cluster of deep white matter that was consistent across pipelines but larger in the TOM8 pipelines and less extensive in the COM pipelines. Fig. 7 illustrates differences in the spatial extent for the white matter cluster for segmentation using the default, TOM8 and COM TPMs (all three shown using the default DARTEL template). The default and COM TPM segmented analyses included a cluster in the corticospinal tract,

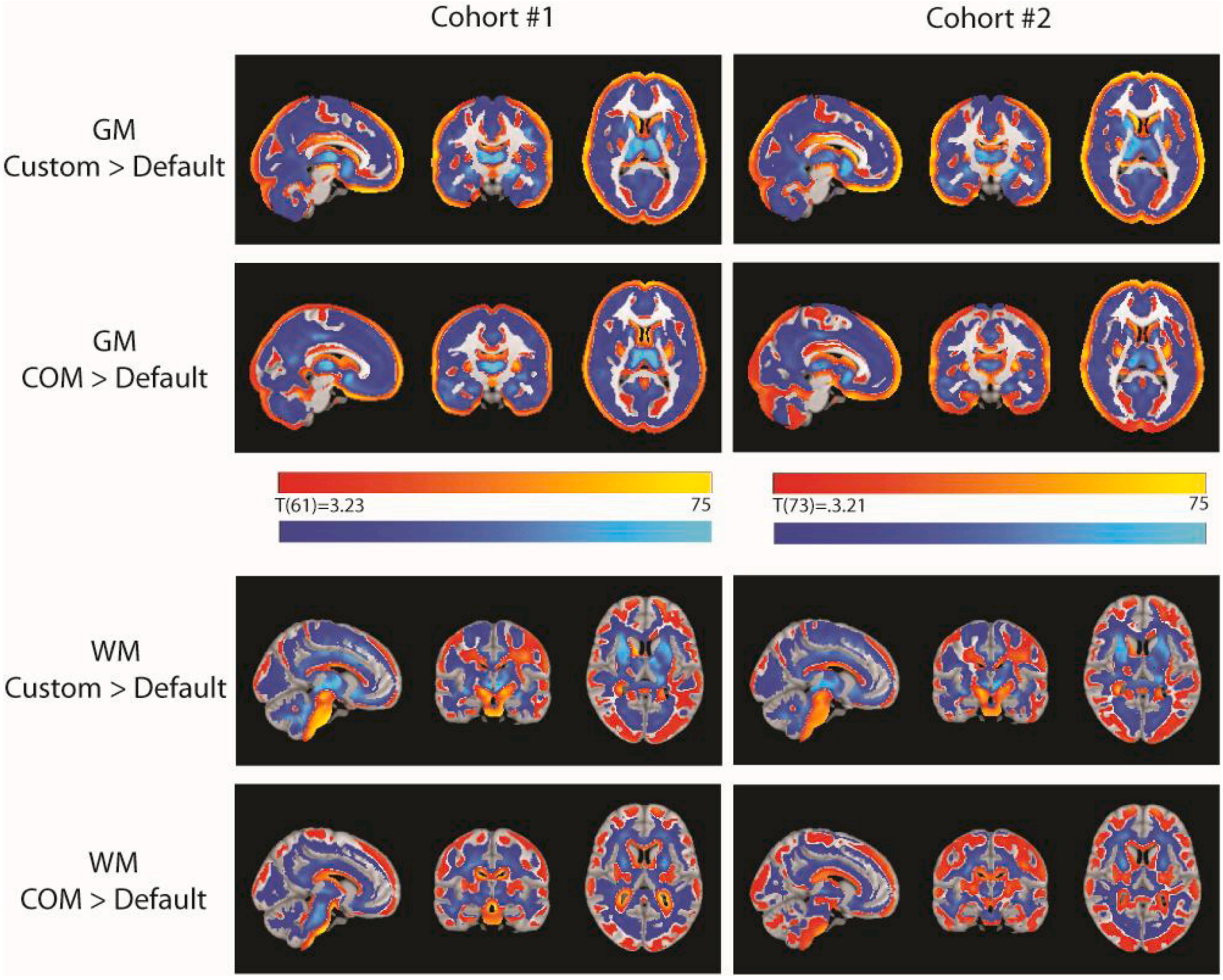

Fig. 4. Significant differences in spatial normalization based on DARTEL template. Within each cohort, paired t-tests compared grey matter (GM) and white matter (WM) images from pipelines using different DARTEL templates, all using the default TPM. Slices shown at [-8 -13 10]; display is radiological. COM = CerebroMatic.

Table 3
Pairwise comparisons of mean volumetric outputs for different TPMs in cohort 2. Paired t-tests were used to compare tissue volume estimates between pairs of pipelines. TPM = tissue probability map. TOM = Template-O-Matic, COM = CerebroMatic.

Measure: TIV						
TPM 1 (cm^3)	TPM 2 (cm^3)	Mean Difference	t(73)	P-value	95 % Confidence Interval for Difference	
					Lower Bound	Upper Bound
Default (1387.94)	TOM (1413.97)	−26.03	−9.68	<.001	−20.67	−31.38
Default (1387.94)	COM (1415.72)	−27.78	−11.18	<.001	−22.82	−32.73
TOM (1413.97)	COM (1415.72)	−1.75	−0.59	= .55	−4.12	7.62
Measure: GM Volume						
TPM 1 (cm^3)	TPM 2 (cm^3)	Mean Difference	t(73)	P-value	95 % Confidence Interval for Difference	
					Lower Bound	Upper Bound
Default (756.25)	TOM (762.86)	−6.61	−2.49	0.014	−1.32	−11.88
Default (756.25)	COM (773.49)	−17.24	−10.17	<.001	−13.86	−20.62
TOM (762.86)	COM (773.49)	−10.64	−5.09	<.001	−6.47	−14.81
Measure: WM Volume						
TPM 1 (cm^3)	TPM 2 (cm^3)	Mean Difference	t(73)	P-value	95 % Confidence Interval for Difference	
					Lower Bound	Upper Bound
Default (418.64)	TOM (425.71)	−7.06	−10.1	<.001	−8.46	−5.67
Default (418.64)	COM (419.04)	−0.39	−0.59	0.56	−1.71	0.93
TOM (425.71)	COM (419.04)	6.67	12.03	<.001	5.57	7.78

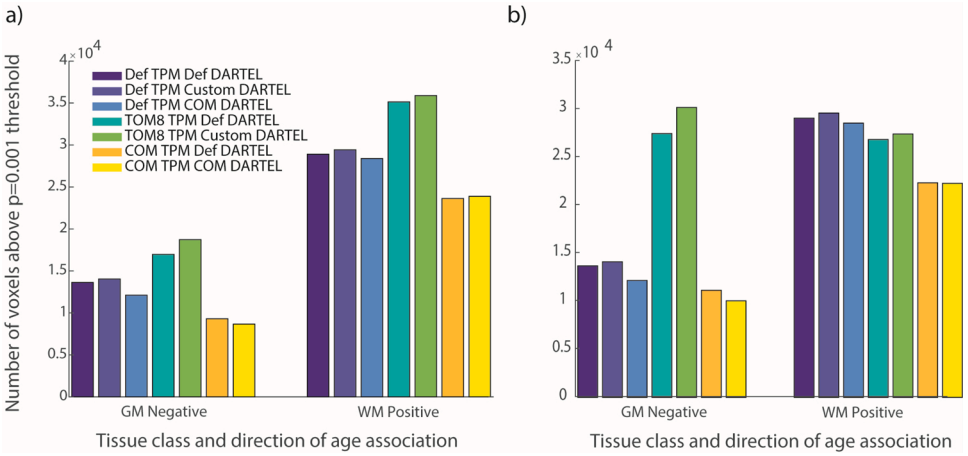

Fig. 5. Number of voxels significantly associated with age for each pipeline. a) With pipeline-specific TIV covariate, b) with consistent default TIV covariate. Pipelines are ordered by TPM, which seemed to have a larger impact on the number of significant voxels than choice of DARTEL template. Across both grey and white matter analyses, the TOM8 TPM showed the largest number of significant voxels and COM TPM the smallest. TOM8=Template-O-Matic, COM = CerebroMatic, GM = grey matter, WM = white matter, Def = default.

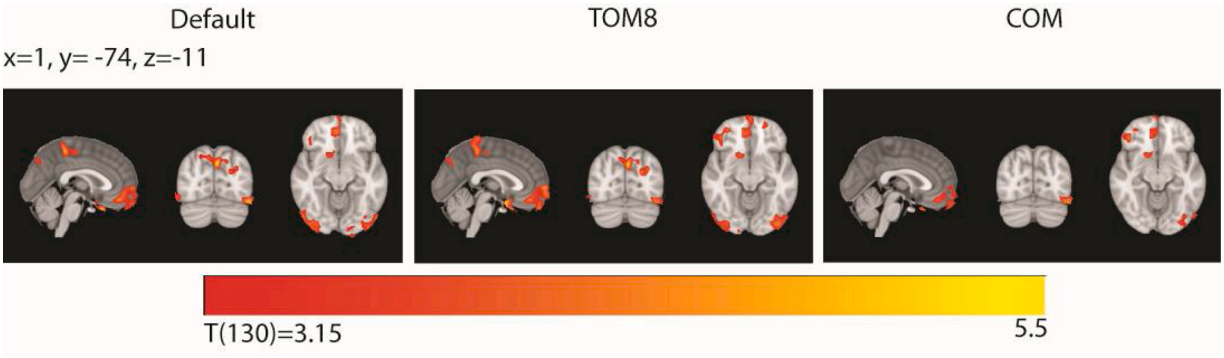

Fig. 6. Grey matter associations with age. Across pipelines, regions showing a significant negative association between grey matter and age ($p < 0.001$ voxel-wise threshold and $p < 0.05$ FDR corrected at the cluster level). While some regions were seen consistently across pipelines (medial prefrontal/oribitofronal, left lateral occipital), other significant regions in the medial parietal and right lateral occipital cortex were only seen in the Default and TOM8 analyses. Panels used the Default, TOM8 or COM TPM and all used the default DARTEL template. Slices shown in radiological convention. TOM8=Template-O-Matic, COM = CerebroMatic.

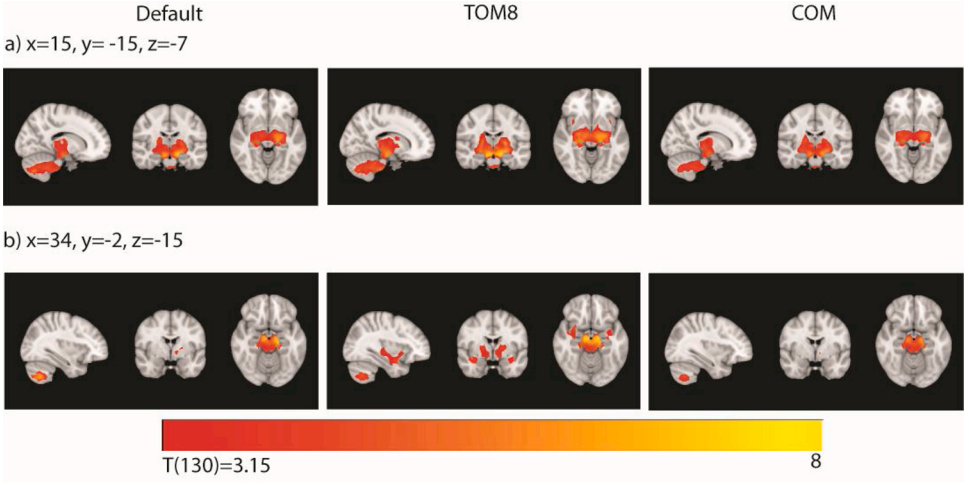

Fig. 7. Positive associations between white matter and age. Across pipelines, regions showing a significant positive association between white matter and age ($p < 0.001$ voxel-wise threshold and $p < 0.05$ FDR corrected at the cluster level). a) Some regions were seen consistently across pipelines (corticospinal tract, cerebellar peduncles, cingulum). b) Other significant regions in the uncinate fasciculus and internal capsule were only seen in the TOM8 analyses. Panels used the Default, TOM8 or COM TPM and all used the default DARTEL template. Slices shown in radiological convention. TOM8=Template-O-Matic, COM = CerebroMatic.

cerebellar peduncles, cingulum and anterior thalamic radiation. This cluster was larger in the TOM8 segmented analysis and extended to include parts of the uncinate fasciculus and inferior frontal occipital fasciculus.

4. Discussion

Custom brain priors and templates seek to improve the sensitivity and validity of VBM studies in populations other than 'typical' young adults, but the influence of pipeline customizations on analysis of data from young children has not been described in detail. Here, we found that the selection of TPM systematically affected tissue classification and statistical inferences drawn by VBM analyses, to a greater extent than the choice of DARTEL template.

Our pipeline comparisons suggest that the choice of TPM can systematically impact tissue classification in a manner that may ultimately

affect the statistical inferences drawn. Relative to default, TPM customization showed differing effects on overall volume estimates, depending on the sample. This in turn influenced the number of statistically significant voxels identified, as seen by comparing models that used consistent or pipeline-specific TIV estimates. However, spatial maps of pipeline-specific differences in grey and white matter volume classification showed similar, TPM-specific, spatial effects across cohorts. Relative to default, the TOM8 TPM led to reduced grey matter classification in sub-cortical regions and increased in ventromedial prefrontal and cuneus. The COM TPM instead showed increased classification of sub-cortical and cortical grey matter, particularly in cohort 2. More accurate classification of sub-cortical grey matter is a notable advantage of the COM TPM.

Although the different pipelines identified the same broad age associations, the number of suprathreshold voxels varied, particularly based on TPM. As this analysis did not have a ground truth, we cannot say whether differences between pipelines represent differences in sensitivity or increased rates of false positives. Thus, whole-brain VBM studies identifying specific regional changes must acknowledge that findings may not be reproducible using different pipeline specifications. Previous work has highlighted that segmentation and normalization procedures may affect the inferences of a VBM study. Callaert et al. previously noted that different VBM pipelines produced different findings of age-related declines in grey matter among adults (Callaert et al., 2014). Although we have compared newer VBM preprocessing options, we nevertheless support their assertion that VBM results across studies may lack comparability if different methods were used.

Our analysis of age associations showed a pattern of increased volume in deep white matter and decreases in select prefrontal, occipital and parietal grey matter regions with age. It has been reported that grey matter development in early childhood is characterized by cortical thinning and increases in surface area, which provide opposing contributions to their resultant volume product (Walhovd et al., 2017). Amlien et al. reported areas of both decreasing and increasing grey matter volumes in 4-year-old children (Amlien et al., 2016), with expanding superior frontal and contracting superior parietal volume extending posteriorly to occipital regions. These identified patterns partially converge with our findings. Amlien et al. reported that overall cortical volume tends to increase until the age of 10, at which point surface area stabilizes while cortical thinning continues (Amlien et al., 2016). Other volumetric studies have reported decreases in grey matter volumes in childhood and adolescence, but many of these regional decreases were reported at an older age than the participants in this study (Krongold et al., 2017; Bray et al., 2015). Among preschool-aged children, some studies report positive grey matter volumetric trajectories in several regions, before decreasing later in childhood and adolescence (Krongold et al., 2017; Bray et al., 2015; Remer et al., 2017). Here, controlling for total intracranial volume, we found only significant negative age-effects in grey matter. A number of factors may influence differences in findings, including age ranges, choice of scaling parameter and image processing pipelines.

Our findings of increased volume in deep white matter converge with previous work from our group in an independent sample (Bray et al., 2015), and with findings of increased fiber cross section in the cortical spinal tract in a sample overlapping with the first cohort reported here (Dimond et al., 2020). Age-associations in deep white matter including the corticospinal tract have also been shown in older children, suggesting protracted maturation beyond the early childhood period (Paus et al., 1999). Notably this finding was consistent across pipelines suggesting that it is relatively robust to differences in processing, while other white matter findings, such as positive age association in anterior parts of the uncinated fasciculus, were only seen in the TOM8 pipeline which had the largest overall white matter volume estimate.

Strengths of this study included systematic comparison of several TPM and DARTEL customization options in a focused early childhood age range. This study also has several limitations to note. As all of the images used in this study were collected on the same MRI scanner, it is unclear how findings might generalize to data collected on other platforms. Furthermore, the sample size may be relatively small to assess subtle grey matter age-associations across a narrow age range. The Template-O-Matic toolbox only allows for a study-specific template to be created for study groups with an average age between aged 4.75–18.58. Thus, Template-O-Matic provides may not be appropriate for pediatric studies investigating younger children. As the average participant age for both of our cohorts was near the minimum cut-off for the Template-O-Matic toolbox, this may have hindered the accuracy of the regression parameters used to generate the TPM. An additional limitation common to all pipelines is the use of registration to the European ICBM template, which is an adult reference. A general limitation of VBM is that it does not allow the separation of volume into cortical thickness and surface area components, which are known to show separable developmental patterns Krongold et al. (2017); Fjell et al. (2018). Although we have demonstrated that study-specific templates and priors influence VBM results, our current pipeline comparisons are relative in nature rather than absolute. As is often the case with neuroimaging analyses, we did not have a ground truth or gold standard that could be used to benchmark the performance of each pipeline, meaning that pipeline selection is subjective. Finally, the localization of white matter volume effects to specific tracts is approximate given that tractography was not performed.

Overall, we have highlighted that the selection of age-appropriate TPMs and DARTEL templates for VBM analysis is an important consideration that can influence statistical results. While our analyses showed negative age associations in grey matter and positive associations in deep white matter, inferences for some regions was different depending on the pipeline used, with the TOM8 TPM leading to the largest number of significant voxels. These differences present a challenge for the field, because we do not have a 'ground-truth' for segmentation of MR images. Understanding the effect of preprocessing is important, because accurate characterization of early childhood brain maturation is necessary to understand the associations between brain changes and the profound social, cognitive and emotional maturation children undergo across this period.

Declaration of Competing Interest

The authors report no declarations of interest.

Acknowledgements

We would like to acknowledge all of the families who gave their time to participate in this work. This research was supported by an NSERC Discovery Grant to SB, a CIHR-INMHA Bridge Grant to SB, a CIHR Operating Grant to CL and a CIHR Project Award to SB.

Appendix A. Supplementary data

Supplementary material related to this article can be found, in the online version, at doi:https://doi.org/10.1016/j.dcn.2020.100875.

References

Altaye, M., Holland, S.K., Wilke, M., Gaser, C., 2008. Infant brain probability templates for MRI segmentation and normalization. Neuroimage 43 (4), 721–730.
Amlien, I.K., Fjell, A.M., Tamnes, C.K., Grydeland, H., Krogsrud, S.K., Chaplin, T.A., et al., 2016. Organizing principles of human cortical development–thickness and area from 4 to 30 years: insights from comparative primate neuroanatomy. Cereb. Cortex 26 (1), 257–267.
Asami, T., Bouix, S., Whitford, T.J., Shenton, M.E., Salisbury, D.F., McCarley, R.W., 2012. Longitudinal loss of gray matter volume in patients with first-episode schizophrenia: DARTEL automated analysis and ROI validation. Neuroimage 59 (2), 986–996.
Ashburner, J., 2007. A fast diffeomorphic image registration algorithm. Neuroimage 38 (1), 95–113.

Ashburner, J., Friston, K.J., 2000. Voxel-based morphometry—the methods. Neuroimage 11, 805–821.
Bergouignan, L., Chupin, M., Czechowska, Y., Kinkingnéhun, S., Lemogne, C., Le Bastard, G., et al., 2009. Can voxel based morphometry, manual segmentation and automated segmentation equally detect hippocampal volume differences in acute depression? Neuroimage 45 (1), 29–37.
Brain Development Cooperative Group, 2012. Total and regional brain volumes in a population-based normative sample from 4 to 18 years: the NIH MRI Study of Normal Brain Development. Cereb. Cortex 22 (1), 1–12.
Bray, S., Dunkin, B., Hong, D.S., Reiss, A.L., 2011. Reduced functional connectivity during working memory in Turner syndrome. Cereb. Cortex 21 (11), 2471–2481.
Bray, S., Krongold, M., Cooper, C., Lebel, C., 2015. Synergistic effects of age on patterns of white and gray matter volume across childhood and adolescence. eNeuro 2 (4). ENEURO.0003-15.2015.
Brown, T.T., Jernigan, T.L., 2012. Brain development during the preschool years. Neuropsychol. Rev. 22 (4), 313–333.
Brown, T.T., Kuperman, J.M., Chung, Y., Erhart, M., McCabe, C., Hagler, D.J.J., et al., 2012. Neuroanatomical assessment of biological maturity. Curr. Biol. 22 (18), 1693–1698.
Callaert, D.V., Ribbens, A., Maes, F., Swinnen, S.P., Wenderoth, N., 2014. Assessing age-related gray matter decline with voxel-based morphometry depends significantly on segmentation and normalization procedures. Front. Aging Neurosci. 6 (124).
Chen, L., Wang, Y., Niu, C., Zhong, S., Hu, H., Chen, P., et al., 2018. Common and distinct abnormal frontal-limbic system structural and functional patterns in patients with major depression and bipolar disorder. Neuroimage Clin. 20, 42–50.
D'Mello, A.M., Crocetti, D., Mostofsky, S.H., Stoodley, C.J., 2015. Cerebellar gray matter and lobular volumes correlate with core autism symptoms. Neuroimage Clin. 7, 631–639.
D'Mello, A.M., Moore, D.M., Crocetti, D., Mostofsky, S.H., Stoodley, C.J., 2016. Cerebellar gray matter differentiates children with early language delay in autism. Autism Res. 9 (11), 1191–1204.
Desikan, R.S., Segonne, F., Fischl, B., Quinn, B.T., Dickerson, B.C., Blacker, D., et al., 2006. An automated labeling system for subdividing the human cerebral cortex on MRI scans into gyral based regions of interest. Neuroimage 31 (3), 968–980.
Dimond, D., Rohr, C.S., Smith, R.E., Dhollander, T., Cho, I., Lebel, C., et al., 2020. Early childhood development of white matter fiber density and morphology. Neuroimage 210, 116552.
Douaud, G., Smith, S., Jenkinson, M., Behrens, T., Johansen-Berg, H., Vickers, J., et al., 2007. Anatomically related grey and white matter abnormalities in adolescent-onset schizophrenia. Brain 130 (Pt 9), 2375–2386.
Fischl, B., 2012. FreeSurfer. Neuroimage 62 (2), 774–781.
Fjell, A.M., Chen, C.-H., Sederevicius, D., Sneve, M.H., Grydeland, H., Krogsrud, S.K., et al., 2018. Continuity and discontinuity in human cortical development and change from embryonic stages to old age. Cereb. Cortex.
Focke, N.K., Trost, S., Paulus, W., Falkai, P., Gruber, O., 2014. Do manual and voxel-based morphometry measure the same? A proof of concept study. Front. Psychiatry 5, 1–7.
Gaser, C., Kurth, F., 2018. Manual: Computational Anatomy Toolbox- CAT12 [Internet]. Available from: http://dbm.neuro.uni-jena.de/cat12/CAT12-Manual.pdf.
Guo, X., Chen, C., Chen, K., Jin, Z., Peng, D., Yao, L., 2007. Brain development in Chinese children and adolescents: a structural MRI study. Neuroreport 18 (June (9)), 875–880.
Hoeft, F., Lightbody, A.A., Hazlett, H.C., Patnaik, S., Piven, J., Reiss, A.L., 2008. Morphometric spatial patterns differentiating boys with fragile X syndrome, typically developing boys, and developmentally delayed boys aged 1 to 3 years. Arch. Gen. Psychiatry 65 (9), 1087–1097.
Hua, K., Zhang, J., Wakana, S., Jiang, H., Li, X., Reich, D.S., et al., 2008. Tract probability maps in stereotaxic spaces: analyses of white matter anatomy and tract-specific quantification. Neuroimage 39 (1), 336–347.
Jernigan, T.L., Trauner, D.A., Hesselink, J.R., Tallal, P.A., 1991. Maturation of human cerebrum observed in vivo during adolescence. Brain 114 (Pt 5), 2037–2049.
Kabani, N., Le Goualher, G., MacDonald, D., Evans, A.C., 2001. Measurement of cortical thickness using an automated 3-D algorithm: a validation study. Neuroimage 13 (2), 375–380.
Klein, A., Andersson, J., Ardekani, B.A., Ashburner, J., Avants, B., Chiang, M.-C., et al., 2009. Evaluation of 14 nonlinear deformation algorithms applied to human brain MRI registration. Neuroimage 46 (3), 786–802.
Krongold, M., Cooper, C., Bray, S., 2017. Modular development of cortical gray matter across childhood and adolescence. Cereb. Cortex 27 (2), 1125–1136.
Kurth, F., Luders, E., Gaser, C., 2015. Voxel-based morphometry. Brain Mapp An Encycl. Ref. 1, 345–349.
Lebel, C., Beaulieu, C., 2011. Longitudinal development of human brain wiring continues from childhood into adulthood. J. Neurosci. 31 (30), 10937 LP–10947 LP.
Lebel, C., Gee, M., Camicioli, R., Wieler, M., Martin, W., Beaulieu, C., 2012. Diffusion tensor imaging of white matter tract evolution over the lifespan. Neuroimage 60 (1), 340–352.
Lenroot, R.K., Gogtay, N., Greenstein, D.K., Wells, E.M., Wallace, G.L., Clasen, L.S., et al., 2007. Sexual dimorphism of brain developmental trajectories during childhood and adolescence. Neuroimage 36 (4), 1065–1073.
Mills, K.L., Lalonde, F., Clasen, L.S., Giedd, J.N., Blakemore, S.-J., 2014. Developmental changes in the structure of the social brain in late childhood and adolescence. Soc. Cogn. Affect. Neurosci. 9 (1), 123–131.
Natu, V.S., Gomez, J., Barnett, M., Jeska, B., Kirilina, E., Jaeger, C., et al., 2019. Apparent thinning of human visual cortex during childhood is associated with myelination. Proc. Natl. Acad. Sci. U. S. A. 116 (41), 20750–20759.
Paus, T., Zijdenbos, A., Worsley, K., Collins, D.L., Blumenthal, J., Giedd, J.N., et al., 1999. Structural maturation of neural pathways in children and adolescents: in vivo study. Science 283 (5409), 1908–1911.
Pergher, V., Demaerel, P., Soenen, O., Saarela, C., Tournoy, J., Schoenmakers, B., et al., 2019. Identifying brain changes related to cognitive aging using VBM and visual rating scales. Neuroimage Clin. 22, 101697.
Reardon, P.K., Seidlitz, J., Vandekar, S., Liu, S., Patel, R., Park, M.T.M., et al., 2018. Normative brain size variation and brain shape diversity in humans. Science 360 (6394), 1222–1227.
Remer, J., Croteau-Chonka, E., Dean 3rd, D.C., D'Arpino, S., Dirks, H., Whiley, D., et al., 2017. Quantifying cortical development in typically developing toddlers and young children, 1-6 years of age. Neuroimage 153, 246–261.
Sowell, E.R., Thompson, P.M., Leonard, C.M., Welcome, S.E., Kan, E., Toga, A.W., 2004. Longitudinal mapping of cortical thickness and brain growth in normal children. J. Neurosci. 24 (38), 8223–8231.
Taki, Y., Thyreau, B., Hashizume, H., Sassa, Y., Takeuchi, H., Wu, K., et al., 2013. Linear and curvilinear correlations of brain white matter volume, fractional anisotropy, and mean diffusivity with age using voxel-based and region-of-interest analyses in 246 healthy children. Hum. Brain Mapp. 34 (8), 1842–1856.
Wakana, S., Caprihan, A., Panzenboeck, M.M., Fallon, J.H., Perry, M., Gollub, R.L., et al., 2007. Reproducibility of quantitative tractography methods applied to cerebral white matter. Neuroimage 36 (3), 630–644.
Walhovd, K.B., Fjell, A.M., Giedd, J., Dale, A.M., Brown, T.T., 2017. Through thick and thin: a need to reconcile contradictory results on trajectories in human cortical development. Cereb. Cortex 27 (2), 1472–1481.
Weise, C.M., Bachmann, T., Schroeter, M.L., Saur, D., 2019. When less is more: structural correlates of core executive functions in young adults – a VBM and cortical thickness study. Neuroimage 189, 896–903.
Whitwell, J.L., 2009. Voxel-based morphometry: an automated technique for assessing structural changes in the brain. J. Neurosci. 29 (31), 9661–9664.
Wierenga, L.M., Langen, M., Oranje, B., Durston, S., 2014. Unique developmental trajectories of cortical thickness and surface area. Neuroimage 87, 120–126.
Wilke, M., 2018. A spline-based regression parameter set for creating customized DARTEL MRI brain templates from infancy to old age. Data Br. 16, 959–966.
Wilke, M., Holland, S., Altaye, M., Gaser, C., 2008. Template-O-Matic: a toolbox for creating customized pediatric templates. Neuroimage 41 (3), 903–913.
Wilke, M., Altaye, M., Holland, S.K., 2017. CerebroMatic: a versatile toolbox for spline-based MRI template creation. Front. Comput. Neurosci. 11, 5.
Xia, Z., Hoeft, F., Zhang, L., Shu, H., 2016. Neuroanatomical anomalies of dyslexia: disambiguating the effects of disorder, performance, and maturation. Neuropsychologia 81, 68–78.
Zielinski, B.A., Prigge, M.B.D., Nielsen, J.A., Froehlich, A.L., Abildskov, T.J., Anderson, J. S., et al., 2014. Longitudinal changes in cortical thickness in autism and typical development. Brain 137 (Pt 6), 1799–1812.